Explicit accumulation model for cyclic loading

A. Niemunis, T. Wichtmann & Th. Triantafyllidis

Institute of Soil Mechanics and Foundation Engineering, Ruhr-University Bochum

ABSTRACT: The essential elements of an explicit model for the accumulation of strain due to cyclic loading are presented. This publication is closely related to the information in two companion papers by Wichtmann et al. (2004b,c). Actually the presented model comprises most of the experimental data given in the above mentioned companion papers. Remarks on the FE implementation and an example of a FE analysis of a strip foundation under cyclic axial load are enclosed.

1 INTRODUCTION

A considerable displacement of structures may be caused by the accumulation of the irreversible deformation of soil due to cyclic loading. If the number of cycles is large then even relatively small amplitudes may endanger the long-term serviceability of structures (especially if its displacement tolerance is small e.g. for a magnetic levitation train). Under undrained conditions, in place of the usual densification, excessive pore pressure is generated. It may lead to soil liquefaction and eventually to a loss of overall stability. Therefore the accumulation phenomenon is of practical importance.

The conventional elastoplastic constitutive models cannot predict any accumulation if the strain loop lies within the elastic regime. Of course, some unintentional accumulation may appear due to numerical errors or a poor, non-conservative elastic stress - strain relation. These errors are often quite considerable also in multisurface elastoplastic models or in the hypoplastic model with intergranular strain (Niemunis 2003) if the number of cycles N exceeds several hundreds. In the present context we say that the classical constitutive models are *implicit* formulations because the accumulation of stress or strain appears as a by-product of calculation by small strain increments. It results from the fact that the loops are not perfectly closed. Implicit strategies require much computation time and magnify systematic errors. For example, 100000 cycles with 100 increments per each cycle increase systematic errors 10^7-times! This requires a constitutive model of unreachable perfection.

The proposed model is based on an alternative *explicit* (Baligh and Whittle 1987) or *N-type* (Sagaseta et al. 1991) formulation. Explicit models are similar to creep laws but in place of the time t the number N of cycles is used. We consider N as a continuous variable, for instance the material "rate" of $\sqcup$ is $\dot{\sqcup} = \mathrm{d}\sqcup / \mathrm{d}N$. Explicit models predict the accumulation due to a bunch of cycles at a time. For example, for $\Delta N = 25$ cycles of amplitude $\gamma^{\mathrm{ampl}} = 0.0001$ we have a direct "explicit" formula to find the resulting irreversible strain.

The following list shows briefly how our explicit model works (the notation is explained in Appendix):

1. Calculate the initial stress state (from self weight and all dead loads) using the hypoplastic model with intergranular strain. Elastic calculation of the initial stress should be avoided because it does not guarantee that all initial stresses will lie within the Coulomb cone.
2. Perform implicitly the first load cycle using the hypoplastic model with intergranular strains and recording the strain path. The recoverable (resilient) part of the deformation is calculated in explicit models in a conventional way (using many strain increments per cycle) in order to estimate the amplitude[1].
3. Estimate the strain amplitude using the recorded

[1] Actually the first two cycles should be calculated. The first (so-called irregular) cycle is very much different from all subsequent ones and is not suitable for the estimation of the representative strain amplitude. The second cycle (= first regular cycle) provides much more reliable information. The accumulation from the implicit calculation of the first two cycles is added to the accumulation from the explicit calculation.

strain path. Having the amplitude we assume that it remains constant over a number of the following cycles.

4. Find the accumulation rate $\mathbf{D}^{\text{acc}}$ of strain using Equation (2)
5. Find the stress increment $\Delta\mathbf{T} = \mathring{\mathbf{T}}\Delta N$ due to a bunch of ΔN cycles

$$\mathring{\mathbf{T}} = \mathsf{E} : (\mathbf{D} - \mathbf{D}^{\text{acc}}) \tag{1}$$

wherein E is the elastic stiffness at average stress $\mathbf{T}^{\text{av}}$. In the calculations E is the linear part of the hypoplastic model with increased shear stiffness as explained in Sec. 4.3.6 of Niemunis (2003). In case of large displacements the Jaumann terms must be added to $\mathring{\mathbf{T}}$. Note that no static load is applied in this phase and the "load increments" are actually packages of ΔN.

The FE program redistributes stress in the course of equilibrium iteration. Depending on the boundary value problem it results in settlements or pseudo-relaxation. It is sometimes practical to interrupt occasionally the above procedure by so-called *control cycles* calculated implicitly. Such cycles are useful to check the admissibility of the stress state, the overall stability (which may get lost if large pore pressures are generated) and, if necessary, to modify the strain amplitude $\boldsymbol{\epsilon}^{\text{ampl}}$ (it may change due to a redistribution of stress). Such an intermitted procedure is sometimes called *semi-explicit*.

The most important part of any explicit model is the expression for the accumulation rate $\mathbf{D}^{\text{acc}}$ caused by a bunch (package) of strain cycles ΔN. A suitable formula can found experimentally for a given strain amplitude and at a given average stress $\mathbf{T}^{\text{av}}$. According to the laboratory tests (Niemunis et al. 2003, Wichtmann et al. 2004a,b,c) the rate of accumulation can be approximated as follows

$$\mathbf{D}^{\text{acc}} \;=\; \mathbf{m}\; f_{\text{ampl}}\; \dot{f}_N\; f_p\; f_Y\; f_e\; f_\pi \tag{2}$$

The unit tensor $\mathbf{m}$ points in the direction of accumulation and the functions $f_{\text{ampl}}, f_N, f_p, f_Y, f_e, f_\pi$ describe the influence of the strain amplitude $\boldsymbol{\epsilon}^{\text{ampl}}$, the number of cycles N, the average stress $p^{\text{av}}, \bar{Y}^{\text{av}}$, the void ratio e, the cyclic strain history and the shape of the strain loop. These function are discussed in the following.

A *cycle* is understood as a repeatable sequence of states recorded during the application and removal of a group of loads. Plotting $\sqcup$ (possibly a tensorial variable) upon a cycle we define its *average* value $\sqcup^{\text{av}} = \frac{1}{2}(\sqcup^{(1)} + \sqcup^{(2)})$ choosing the pair (1,2) of instantaneous values in such way that their distance reaches a maximum, $\| \sqcup^{(1)} - \sqcup^{(2)} \| = \max \| \sqcup^{(i)} - \sqcup^{(j)} \|$. In other words, $\sqcup^{\text{av}}$ is the centre of the smallest "sphere" that encompasses all states $\sqcup$ of a given cycle. The scalar amplitude is defined as $\sqcup^{\text{ampl}} = \max \| \sqcup - \sqcup^{\text{av}} \|$. A more elaborated definition of a tensorial amplitude (including polarization and openness of the strain loop) is proposed in Section 3.

Note that the unspecified term *accumulation* is a convenient notion that expresses both cyclic pseudo-relaxation and cyclic pseudo-creep. They are just different manifestations of the same physical phenomenon. If stress cycles are applied we observe cyclic pseudo-creep and if strain cycles are applied we obtain cyclic pseudo-relaxation. It is thus natural to speak of accumulation (a physical phenomenon) independently of its appearance, i.e., independently of the technical aspect how the experiment was controlled. Moreover, many testing devices allow for mixed control so pseudo-relaxation and pseudo-creep occur simultaneously but in different directions.

It turns out that the phenomenon of accumulation depends strongly on several subtle properties of soil (distribution of grain contact normals, arrangement of grains) which cannot be expressed by the customary state variables (stress and void ratio) only. Therefore some new structural variables will be proposed. The initial values of the new state variables are somewhat unclear, as discussed by Triantafyllidis et al. (2004).

Numerous explicit constitutive models proposed in the literature (Barksdale 1972, Lentz & Baladi 1981, Khedr 1985, Paute et al. 1988, Hornych et al. 1993, Sweere 1990, Wolff & Visser 1994, Vuong 1994, Sawicki 1987, Martin et al. 1975, Bouckovalas et al. 1984, Marr & Christian 1981, Suiker 1998, 1999, Gotschol 2002) are usually strongly simplified because cyclic tests are much more laborious than the conventional ones and it is difficult to collect a sufficient amount of experimental data. The authors have often very specific applications and very special kinds of loading in mind, e.g., considering volumetric accumulation, constant average stress $\mathbf{T}^{\text{av}}$, linear amplitudes only (in general the openness and the polarization of the strain loop may be of importance).

At the beginning of our research we chose a simple and elegant explicit model from the literature (Sawicki & Świdziński 1989, Sawicki 1991) and combined it with K-hypoplasticity (Gudehus 1996, Kolymbas 2000), a constitutive model alternative to elastoplasticity. The original accumulation was purely volumetric, $m_{ij} = -\frac{1}{\sqrt{3}}\delta_{ij}$, and neglected the influence of stress $f_p = f_Y = 1$ and changes of the void ratio. The only state variable was the number of cycles scaled by the square of the (scalar) amplitude of the deviatoric strain, $\tilde{N} = \frac{1}{2}\|\boldsymbol{\epsilon}^{*\ \text{ampl}}\|^2 N$, so that

$$f_{\text{ampl}}\dot{f}_N = \frac{C_1 C_2}{1 + C_2\tilde{N}} \tag{3}$$

and $C_1(e_0), C_2(e_0)$ were parameters related to the initial void ratio e_0. In the course of our study we were

modifying this model as new results were coming from the laboratory (mainly triaxial and multiaxial DSS tests). Now, after a four-year study there is actually not much left of the original formulation (and of its simplicity).

2 ELEMENTS OF THE MODEL

The factors appearing in (2) are discussed briefly further in this text. They are closely related to the experimental evidence presented in the three companion papers (Wichtmann et al. 2004b,c, Triantafyllidis et al. 2004) referred as CPTX, CPMX and CPH, respectively.

2.1 *Direction of accumulation* **m**

The rate of strain accumulation $\mathbf{D}^{\text{acc}}$ is not purely volumetric. A significant deviatoric accumulation was reported in the literature (Suiker 1999). Judging by the triaxial compression and triaxial extension tests presented in CPTX, the direction of accumulation **m** is well described by the flow rule taken from the hypoplastic model. For a particular version (Wolffersdorff 1996, Wolffersdorff 1997) of hypoplasticity

$$\mathbf{m} \sim -\left[\left(\frac{F}{a}\right)^2 (\hat{\mathbf{T}} + \hat{\mathbf{T}}^*) + \hat{\mathbf{T}} : \hat{\mathbf{T}}\hat{\mathbf{T}}^* - \hat{\mathbf{T}}\hat{\mathbf{T}} : \hat{\mathbf{T}}^*\right] \quad (4)$$

where the right-hand side should be normalized and where F and a are given in Appendix.

In particular, for $\mathbf{T}^{\text{av}}$ beyond the critical state line (CSL given by φ_c) the void ratio can increase! In consequence, in the course of a pseudo-relaxation process stress does not surpass the limit surface. FE results were decisively improved after the deviatoric component of accumulation had been added (the predicted settlements were larger). The direction of the accumulation was observed to be independent of the void ratio and to become slightly more volumetric with N (CPTX). This tendency, however, must reverse because at the maximum density further densification is inadmissible and only deviatoric deformations may take place. Provisionally we assume that **m** is a function of stress ratio $\hat{\mathbf{T}}$ only. The direction **m** does not depend on the polarization of the amplitude: for cyclic triaxial compression and for cyclic isotropic compression similar directions **m** have been measured, cf. Figure 13 in CPMX and Figure 19 in CPTX.

2.2 *Scalar amplitude and number of cycles*

In this subsection we consider *in-phase* (IP = *proportional*) strain cycles which can be defined by the equation

$$\boldsymbol{\epsilon} = \boldsymbol{\epsilon}^{\text{av}} + \boldsymbol{\epsilon}^{\text{ampl}} f(t) \quad (5)$$

which means that all components oscillate along with the same scalar periodic function, e.g. $f(t) = \sin(t)$, varying between -1 an 1 and using a time-like parameter t. In *uniaxial* cycles the tensor $\boldsymbol{\epsilon}^{\text{ampl}}$ has only one non-zero component, e.g. $\epsilon_{11}^{\text{ampl}} \neq 0$, otherwise we speak of *multiaxial* cycles. The out-of-phase (OOP) amplitudes do not satisfy (5) and are discussed separately in Section 3.

The experiments (Figure 7 in CPTX) show that the accumulation rate is proportional to the square of the strain amplitude. It is evident from Figure 8 in CPTX that the accumulated strain cannot be described as a unique function of $\tilde{N}$, as proposed in Equation (3). Therefore, in order to consider the size of the amplitude we should look for the second order homogeneous function $\mathbf{D}^{\text{acc}}(n\epsilon^{\text{ampl}}, \ldots) = n^2 \mathbf{D}^{\text{acc}}(\epsilon^{\text{ampl}}, \ldots)$. The following simple expression has been chosen

$$f_{\text{ampl}} = \left(\frac{\epsilon^{\text{ampl}}}{\epsilon_{\text{ref}}^{\text{ampl}}}\right)^2 \quad (6)$$

The reference amplitude is $\epsilon_{\text{ref}}^{\text{ampl}} = 0.8165\ 10^{-4}$. This formula is suitable for purely deviatoric deformations, $\boldsymbol{\epsilon}^{\text{ampl}} = \boldsymbol{\epsilon}^{*\text{ampl}}$ with $\epsilon^{\text{ampl}} = \|\boldsymbol{\epsilon}^{*\text{ampl}}\|$, only. If the amplitude $\boldsymbol{\epsilon}^{\text{ampl}}$ of strain contains a volumetric portion we must treat the volumetric and the deviatoric portions separately. The volumetric part of the amplitude contributes less to the accumulation rate than the deviatoric one, cf. Section 2.3 in CPMX. One *cannot* just substitute $\epsilon^{\text{ampl}} = \|\boldsymbol{\epsilon}^{\text{ampl}}\|$ into (6). Instead of (6) we propose an alternative definition of f_{ampl}. Using isomorphic components (see Appendix) of the strain amplitude ϵ_P^{ampl} and ϵ_Q^{ampl}, the expression for f_{ampl} takes the form

$$f_{\text{ampl}} = \left(\frac{\epsilon_Q^{\text{ampl}} + C_{\text{ampl}} \epsilon_P^{\text{ampl}}}{\epsilon_{\text{ref}}^{\text{ampl}}}\right)^2 \quad (7)$$

with the material constant $C_{\text{ampl}} \approx 0.5$, see Section 2.3 in CPMX.

Having f_{ampl} all experimental accumulation curves from Figure 6 in CPTX can be described by a common function f_N consisting of a linear and a logarithmic part. The rate form of f_N is

$$\dot{f}_N \;=\; \frac{C_{N1} C_{N2}}{1 \,+\, C_{N2}\, N} \,+\, C_{N1}\, C_{N3}\,. \quad (8)$$

Figure 31 in CPTX shows that expression (8) sufficiently well approximates the experimental data. Equation (8) is similar to (3) except for the linear term $C_{N1}C_{N3}$.

Unfortunately, the product $f_{\text{ampl}}\dot{f}_N$ which describes so well all experimental curves with the number N of cycles in (8) memorized by the material as a state variable is *not* suitable for our purposes. Such formulation

severely contradicts the Miner's rule (Miner 1945). Although this rule concerns the fatigue of metals (generalizes the Wöhler's curve) it seems applicable also to sands. The Wöhler's SN-curve tells the number N_f of uniaxial cycles of a constant stress amplitude $S = T_1^{\text{ampl}}$ that causes failure and the (Palmgren-)Miner's rule describes the effect of uniaxial block-periodic cycles (with a constant amplitude within each block). Suppose we have several amplitudes S_i with the corresponding numbers of cycles to failure $N_{f\,i}$ and the number of applied cycles n_i then the Miner's rule can be expressed by inequality

$$\sum_{i=1}^{n} \frac{n_i}{N_{f\,i}} < 1 \tag{9}$$

The most important implications of the Miner's rule for sand are

- the sequence of application of constant-amplitude blocks is of no importance
- the periodic strain loop can be decomposed into several *convex* loops using the so-called rainflow algorithm. These convex loops can be applied sequentially as separate loading processes.

Before a closer examination of the inconsistency between (8) and (9) (in order to find a better state variable than N) let us examine whether the proposition (3) satisfies the Miner's rule. Integrating (3) with the initial value $\tilde{N} = \tilde{N}_0$ we obtain

$$f_{\text{ampl}} f_N = C_{N1} \Big[\ln(1 + C_{N2}(\Delta\tilde{N} + \tilde{N}_0)) - \ln(1 + C_{N2}\tilde{N}_0)\Big] \tag{10}$$

The sequence of application of packages $\Delta\tilde{N}_1$ and $\Delta\tilde{N}_2$, each with a different constant amplitude, is of no importance because in both cases the final integral is

$$f_{\text{ampl}} f_N = C_{N1} \Big[\ln(1 + C_{N2}(\Delta\tilde{N}_1 + \Delta\tilde{N}_2 + \tilde{N}_0)) - \ln(1 + C_{N2}\tilde{N}_0)\Big] \tag{11}$$

and thus the Miner's rule is satisfied. One may ask whether sands obey the Miner's rule so rigorously, especially if the packages have different polarization. However, in one special case the Miner's rule must be obeyed, namely for a combination of ΔN_1 cycles with $\boldsymbol{\epsilon}_1^{\text{ampl}}$ and ΔN_2 with $\boldsymbol{\epsilon}_2^{\text{ampl}} \to 0$. The final accumulation should be independent of the sequence of application of these packages because it should not matter whether we *do nothing* after or before application of ΔN_1 cycles with $\boldsymbol{\epsilon}_1^{\text{ampl}}$. The cycles ΔN_2 should have no effect. Evidently, for (8) this is not the case. Therefore the number N of cycles is not a suitable state variable. From this point of view $\tilde{N}$ is a better alternative, but it fits poorly the experimental results. In order to solve this dilemma let us rewrite (8) in an alternative form with a novel state variable in place of N. First let us abbreviate $\dot{g} = f_{\text{ampl}}\ \dot{f}_N$ given by (8) and (7) and integrate this product within the limits N_0 and $N = N_0 + \Delta N$ and between g_0 and g. We obtain

$$g = f_{\text{ampl}} C_{N1} \left[\ln\left(1 + C_{N2}N\right) + C_{N3}N\right] \tag{12}$$

with the initial value

$$g_0 = f_{\text{ampl}} C_{N1} \left[\ln\left(1 + C_{N2}N_0\right) + C_{N3}N_0\right]. \tag{13}$$

The variable $g = g^A + g^B$ can be decomposed into the part g^A related to the adaptation of the structure of the material and the linear part g^B which becomes dominant for large numbers of cycles:

$$g^A = f_{\text{ampl}} C_{N1} \ln(1 + C_{N2}N) \tag{14}$$

$$g^B = f_{\text{ampl}} C_{N1} C_{N3} N \tag{15}$$

with $g_0^A = f_{\text{ampl}} C_{N1} \ln(1 + C_{N2}N_0)$ and $g_0^B = f_{\text{ampl}} C_{N1} C_{N3} N_0$ being the respective initial values. Our model uses rates so analogously we may write

$$\dot{g}^A = f_{\text{ampl}} \frac{C_{N1} C_{N2}}{1 + C_{N2}N} \tag{16}$$

$$\dot{g}^B = f_{\text{ampl}} C_{N1} C_{N3} \tag{17}$$

Note that the linear part $\dot{g}^B$ requires no memory of the material whereas the 'structural' part $\dot{g}^A$ depends on N. However, we do not want N to be a state variable. The idea is to replace N in (16) by g^A. The advantage of such a replacement is that g^A contains information about N and additionally about the amplitudes of cycles in the past. For our purpose we solve (14) for N and substitute the result into (16) obtaining

$$\dot{g}^{\,A} = f_{\text{ampl}} C_{N1} C_{N2} \exp\left[-\frac{g^A}{C_{N1} f_{\text{ampl}}}\right] \tag{18}$$

This equation is equivalent to (16) only if the amplitude remains constant. For the above mentioned special case (with $\boldsymbol{\epsilon}_2^{\text{ampl}} \to 0$) the Miner's rule is obeyed. A numerical simulation of the accumulation due to two blocks of cycles with different amplitudes and applied in different sequences is shown in Figure 1. The physical interpretation of $g^A - g_0^A$ is simply the norm of the accumulated strain at $f_p\ \ f_Y\ \ f_e\ \ f_\pi = 1$ diminished by the basic accumulation $g^B = \int_{N'=0}^{N} f_{\text{ampl}} C_{N1} C_{N3} \mathrm{d}N'$. The problem of the determination of the initial value g_0^A is the subject of the separate paper CPH. Unfortunately, the question of the initial values of the state variables in explicit models is rarely discussed in the literature.

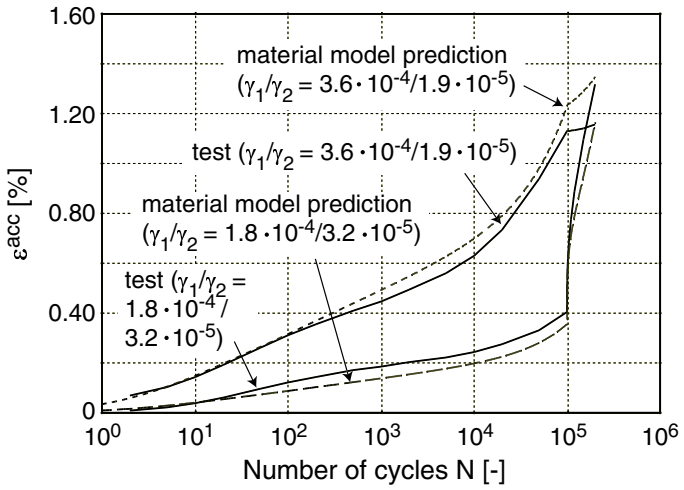

Figure 1. Numerical calculation and experimental verifi cation of the Miner's rule. Strain amplitudes are denoted as γ_1 and γ_2

2.3 *Average stress and void ratio*

The rate of accumulation measured in the triaxial tests shown in CPTX depend on stress ratio $\hat{\mathbf{T}}$ and on the mean stress p. It is convenient to treat these effects separately using the functions f_Y and f_p, respectively. The rate of accumulation increases strongly with the stress ratio $\eta = q/p$, especially if η is close to the critical state line (CSL). This dependence can be described using a well-known stress function proposed in the literature (Matsuoka & Nakai 1982) as a yield criterion. The observed accumulation rate increases according to the following empirical function

$$f_Y = \exp(C_Y \bar{Y}^{\text{av}2}) \quad \text{with} \quad C_Y \approx 2\,. \tag{19}$$

wherein

$$\bar{Y} = \frac{Y - 9}{Y_c - 9} \tag{20}$$

$$Y = -\frac{I_1 I_2}{I_3} \tag{21}$$

$$Y_c = \frac{9 - \sin^2\varphi_c}{1 - \sin^2\varphi_c} \tag{22}$$

The stress invariants I_1, I_2, I_3 are defined in Appendix and the critical friction angle is denoted by φ_c. Equation (19) is based on numerous triaxial compression and extension tests, cf. CPTX.

Increasing the mean effective stress p the accumulation rate becomes smaller, viz.

$$f_p = \exp\left[-C_p\,\left(\frac{p^{\text{av}}}{p_{\text{atm}}} - 1\right)\right] \tag{23}$$

wherein $p_{\text{atm}} = 100$ kPa and the material constant is $C_p \approx 0.44$. The experimental evidence is given in Section 5.2 of CPTX.

Of course loose sands have higher densification rates than dense ones. The following empirical dependence was found, cf. Section 5.3 of CPTX

$$f_e = \frac{(C_e - e^{\text{av}})^2}{1 + e^{\text{av}}} \frac{1 + e^{\text{av}}_{\text{ref}}}{(C_e - e^{\text{av}}_{\text{ref}})^2} \tag{24}$$

wherein the parameters $e^{\text{av}}_{\text{ref}} = 0.874$ and $C_e = 0.52$ correspond to medium coarse uniform sand. The interesting observation can be made that the dependence of the accumulation rate on pressure and void ratio cannot (Niemunis et al. 2003) be captured collectively using the relative density $r_e = (e - e_d)/(e_c - e_d)$ wherein $e_d(p)$ and $e_c(p)$ are the pressure-dependent minimum and critical void ratios. Keeping $r_e = \text{const}$ the rate of cyclic accumulation was observed to be almost proportional to p^{-1} (for $N = 10^5$), i.e. $\mathbf{D}^{\text{acc}}$ decreases(!) with p. This means that pairs (p, e) of identical cyclic rate of accumulation may lie even on different sides of the critical state line $e_c(p)$ usually described by the inclination λ in the $e - \log p$ diagram, see Figure 2

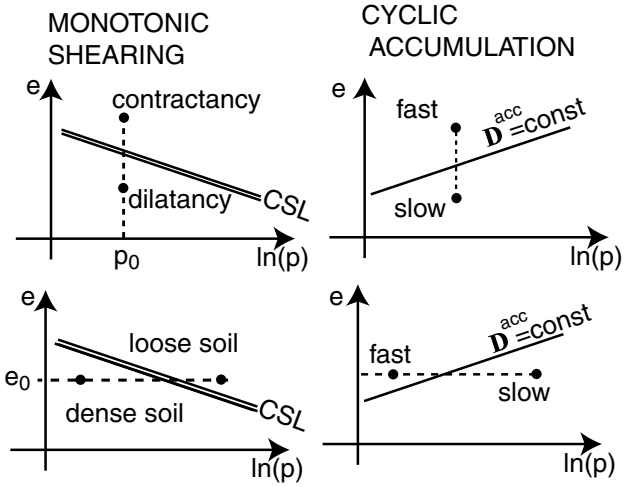

Figure 2. Lines of constant rate of accumulation in $e - \log p$ diagram are differently inclined than the CSL

3 OUT-OF-PHASE CYCLES

An interesting element of the explicit description of accumulation is the consideration of the shape (openness) of the strain cycle. A similar effect is also studied in the fatigue of metals (Ekberg 2000, Papadopoulos 1994). As already mentioned, the in-phase (IP) cycles satisfy (5), whereas the out-of-phase (OOP) cycles do not, for example an OOP strain cycle can be given by the function

$$\boldsymbol{\epsilon}(t) = \boldsymbol{\epsilon}^{\text{av}} + \begin{pmatrix} \epsilon_{11}^{\text{ampl}} \sin t & 0 & 0 \\ 0 & \epsilon_{22}^{\text{ampl}} \sin(t + \frac{\pi}{2}) & 0 \\ 0 & 0 & 0 \end{pmatrix} \tag{25}$$

An OOP strain loop encloses some volume in the strain space. It turns out that OOP cycles produce more accumulation than IP cycles of the same *scalar* amplitude, but less than the total effect of all IP cycles obtained from the OOP loop by spectral decomposition, cf. Section 2.4 in CPMX. Using the example (25) let us assume that $\epsilon_{11}^{\text{ampl}} > \epsilon_{22}^{\text{ampl}} > 0$. For the phase-shift $t_0 = \frac{\pi}{2}$ the scalar amplitude is simply $\epsilon^{\text{ampl}} = \epsilon_{11}^{\text{ampl}}$. It can be stated (analogously to observations in Section 2.4 in CPMX) that N elliptical loops defined by (25) produce more accumulation than N uniaxial cycles with $\epsilon_{11}^{\text{ampl}}$ but less accumulation than N uniaxial cycles with $\epsilon_{11}^{\text{ampl}}$ followed by N uniaxial cycles with $\epsilon_{22}^{\text{ampl}}$. Another phenomenon shown experimentally in Section 3.1 of CPMX is an increase of the rate of accumulation after a sudden change of the orientation of the polarization i.e. the orientation of the main axis along which cycles are performed. This effect is described in the following using a so-called 'back polarization'.

In order to consider the openness and the polarization of strain cycles a novel definition of amplitude is introduced. The amplitude A_ϵ is proposed to be a sum of dyadic products $\mathbf{r}^i\mathbf{r}^i$ of the unit tensors $\mathbf{r}^i$ which are pointing along the maximum spans of the strain path (loop) in the six dimensional strain space. The directions of spans are mutually orthogonal, i.e. $\mathbf{r}^i : \mathbf{r}^j = \delta_{ij}$ with $i, j = 1, \ldots, 6$, and each dyad is multiplied by a perimeter of a specially chosen projection of the strain loop.

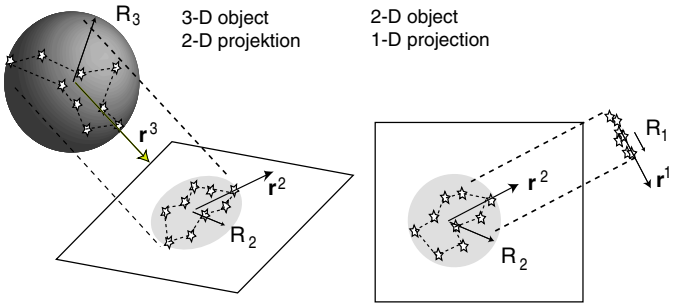

Figure 3. The directions $\mathbf{r}_i$ and the sizes R_i of the strain loop amplitude

Suppose that we are given a simple strain loop (a more or less closed strain path without sub-loops). At first it is given in form of a sequential list of discrete strains $\boldsymbol{\epsilon}_k$, $k = 1, \ldots, M$ recorded by a FE program along the loop for each Gauss point. These strain states lie in a 6-D strain space and need not be coaxial. For example, rotation of the principal directions of strain also generates a loop. Usually the strain loops are smaller than 0.1 % so small strain theory can be used. The following steps demonstrate how the subsequent projections of the strain loop, their radii and perimeters are calculated. Later they will enter the definition of the tensorial amplitude. The upper index indicates the number of dimensions of the strain space which is considered.

1. Flatten the volumetric size of the loop, so that the size ϵ_P^{ampl} becomes C_{ampl} times smaller. We do so because the volumetric portion of the strain amplitude contributes less than the deviatoric one.
2. Calculate the perimeter $P_6 = \sum_{i=1}^{M} \|\boldsymbol{\epsilon}^6(t_i) - \boldsymbol{\epsilon}^6(t_{i-1})\|$ of the loop[2] wherein M denotes the number of recorded strain states upon the loop.
3. Find the middle point $\boldsymbol{\epsilon}_{\text{av}}^6$ of the smallest 6-D (hyper)sphere that encompasses the loop[3].
4. Calculate the unit tensor $\mathbf{r}^6$ pointing from $\boldsymbol{\epsilon}_{\text{av}}^6$ to the most distant point $\boldsymbol{\epsilon}^6(t_i)$ of the loop. Usually there are two points (antipodes) "most distant" from $\boldsymbol{\epsilon}_{\text{av}}^6$. We may choose $\mathbf{r}^6$ towards any of them because the sign of $\mathbf{r}^i$ is of no importance.
5. Project the loop onto the (hyper)plane perpendicular to $\mathbf{r}_6$ calculating $\boldsymbol{\epsilon}^5(t_i) = \boldsymbol{\epsilon}^6(t_i) - \mathbf{r}^6 : \boldsymbol{\epsilon}^6(t_i)\mathbf{r}^6$.
6. Find the perimeter $P_5 = \sum_{i=1}^{M} \|\boldsymbol{\epsilon}^5(t_i) - \boldsymbol{\epsilon}^5(t_{i-1})\|$.
7. Find the middle point $\boldsymbol{\epsilon}_{\text{av}}^5$ of 5-D (hyper)sphere that encompasses the projected 5-D loop.
8. Analogously find the unit tensor $\mathbf{r}^5$ and the projection $\boldsymbol{\epsilon}^4(t_i) = \boldsymbol{\epsilon}^5(t_i) - \mathbf{r}^5 : \boldsymbol{\epsilon}^5(t_i)\mathbf{r}^5$. Using the new projection find $P_4, \mathbf{r}^4$ and then $P_3, \mathbf{r}^3$ etc.

Reduction steps from the 3-dimensional path to the 1-dimensional path are shown in Figure 3. After a series of projections a list of perimeters P_D and orientations $\mathbf{r}^D$ is calculated for the dimensions $D = 1 \ldots 6$. The orientations are all mutually perpendicular $\mathbf{r}^i : \mathbf{r}^j = \delta_{ij}$ and inequalities $P_D \geq P_{D-1}$ hold.

The sense of the orientation $\mathbf{r}^D$ must not enter the definition of the amplitude. Therefore the dyadic products $\mathbf{r}^D\mathbf{r}^D$ are used. Their weighted sum

$$\mathsf{A}_\epsilon = \frac{1}{4}\sum_{D=1}^{6} P_D \mathbf{r}^D\mathbf{r}^D \tag{26}$$

is proposed to be the definition of the amplitude. The unit amplitude

$$\vec{\mathsf{A}}_\epsilon = \mathsf{A}_\epsilon / \|\mathsf{A}_\epsilon\| \tag{27}$$

is called *polarization*. If a package of cycles with the amplitude $\mathsf{A}_\epsilon{}^1$ is directly followed by another package with $\mathsf{A}_\epsilon{}^2$ such that $\vec{\mathsf{A}}_\epsilon{}^1 :: \vec{\mathsf{A}}_\epsilon{}^2 = 1$, the polarizations are identical and no additional increase of the accumulation rate should be generated. However, for $0 < \vec{\mathsf{A}}_\epsilon{}^1 :: \vec{\mathsf{A}}_\epsilon{}^2 < 1$ the rate of accumulation (cyclic creep/relaxation) should be increased.

[2] Defi ne $\boldsymbol{\epsilon}^6(t_0) = \boldsymbol{\epsilon}^6(t_M)$ to close the loop.

[3] Numerically more convenient (although less accurate) is determination of two most distant strains (largest span of the loop) and choosing $\boldsymbol{\epsilon}_{\text{av}}$ to be their mean value.

3.1 *Function* f_π

As shown by experiments in CPMX the phenomenon of adaptation of soil structure to cyclic loading should be taken into account. This section presents a draft implementation of the effect of polarization changes. The polarization integrated over the recent cyclic history is called *back polarization* $\boldsymbol{\pi}$. Its evolution equation and a special correction function f_π will be postulated to account for the difference between the current polarization $\vec{\mathsf{A}}_\epsilon$ and the recent polarization $\boldsymbol{\pi}$. The degree of adaptation of the material structure to the polarization of the current cyclic loading is expressed by the product $0 \leq \boldsymbol{\pi} :: \vec{\mathsf{A}}_\epsilon \leq 1$. The upper and lower limits correspond to full adaptation (= slow accumulation) and to a complete lack of adaptation (= fast accumulation), respectively. During cycles with $\vec{\mathsf{A}}_\epsilon = \text{const}$ (let us call such loading *c-monotonic*) adaptation is described by the evolution of $\boldsymbol{\pi}$ which tends towards the current polarization, $\boldsymbol{\pi} \to \vec{\mathsf{A}}_\epsilon$. This process manifests itself as a decrease of the accumulation rate and can be expressed by the following evolution equation:

$$\dot{\boldsymbol{\pi}} \;=\; C_{\pi 3}\left(\vec{\mathsf{A}}_\epsilon - \boldsymbol{\pi}\right)\|\mathsf{A}_\epsilon\|^2 \qquad (28)$$

Back polarization tends towards the polarization of the current amplitude $\boldsymbol{\pi} \to \vec{\mathsf{A}}_\epsilon$ because $C_{\pi 3}$ is positive. An increase in the rate of accumulation is proposed to be described by

$$f_\pi \;=\; 1 + C_{\pi 1}\left[1 - \left(\vec{\mathsf{A}}_\epsilon :: \boldsymbol{\pi}\right)^{C_{\pi 2}}\right]. \qquad (29)$$

The determination of the material constants in our hypothetical model is presented with examples in Section 3.1 of CPMX.

Let us examine briefly the properties of the polarization tensor. A special case of perfect polarization can be generated by a long c-monotonic package of IP cycles. In 6-D strain space $\left\{\epsilon_{11}, \epsilon_{22}, \epsilon_{33}, \sqrt{2}\epsilon_{12}, \sqrt{2}\epsilon_{13}, \sqrt{2}\epsilon_{23}\right\}$ we obtain a 6×6 dyadic matrix

$$\boldsymbol{\pi} = \vec{\mathsf{A}} = \vec{\mathbf{r}}\;\vec{\mathbf{r}} \qquad (30)$$

It has the spectrum $\{0,0,0,0,0,0,0,0,1\}$ with the eigenvector $\vec{\mathbf{r}}$ corresponds to the non-zero eigenvalue.

If the cyclic prestraining is perfectly chaotic then the back polarization is proportional to the mean value of $\vec{\mathbf{r}}\,\vec{\mathbf{r}}$ over all directions in the 6-D space. This mean value can be found from integration of $\vec{\mathbf{r}}\,\vec{\mathbf{r}}$ over all directions in the 6-D space and dividing the result by the surface $S^{6D} = \pi^3$ of the unit 6-D hypersphere. The result is $\frac{1}{6}J^{6D}$ where J^{6D} denotes the 6-D identity matrix. In order to obtain an isotropic tensorial polarization we must just normalize the analogous result

Function	typical range	remarks
f_{ampl}	$0 \ldots 2500$	use (7)
$\dot{f}_N$	$(0.1 \ldots 0.2)\ 10^{-3}$	$0 < N < \infty$
f_p	$1.5 \ldots 0.02$	$10 < p < 1000$ kPa
f_Y	$1 \ldots 7.4$	$0 < \bar{Y} < 1$
f_e	$1 \ldots 0.06$	$e_{\text{ref}} > e > 0.6$
f_π	$1 \ldots 4$	quickly declines

Table 1. Variability of different functions in (2)

obtaining

$$\boldsymbol{\pi}^{\text{ISO}} = \frac{1}{3}\mathsf{J} \qquad (31)$$

wherein J is given in Appendix. Not knowing much about the history of a sample we may want to choose such isotropic state $\boldsymbol{\pi} = \boldsymbol{\pi}^{\text{ISO}}$, to be the initial value. It means that no orientation of the amplitude is preferred.

4 SENSITIVITY of $\mathbf{D}^{\text{acc}}$

In the previous sections we have presented effects that influence the rate of accumulation. One by one they were studied first in the laboratory and then simple functions were formulated which approximate the observations. The results are summarized in Table 1 in CPTX. However some readers may ask whether all factors listed in this table are indeed necessary in the model. Determination of their parameters may require a considerable effort. Therefore the Table 1 in CPTX will be now supplemented by Table 1 in this paper showing the expected variability of the functions $f_{\text{ampl}}, \dot{f}_N, f_p, f_Y, f_e, f_\pi$ for the typical range of input parameters. Table 1 shows that all factors examined in the experimental part of our research may strongly influence the rate of accumulation and their incorporation to the model seems justified.

5 FE IMPLEMENTATION

The semi-explicit model has been implemented to the FE-program ABAQUS in the form of a user's material subroutine. An alternative computation algorithm (not requiring ABAQUS) is presented by Niemunis (2000). The constitutive subroutine UMAT has three modes of operation:

1. *Implicit mode* passes the control to the conventional hypoplastic constitutive model. This mode is used

to find the initial state equilibrium and to perform irregular cycles.

2. *Recording mode* is also an implicit mode but the strain states the program is going through are memorized for the future calculation of the amplitude. Of course only characteristic states are written down to reduce the memory consumption. For this purpose some filtering criteria, e.g. $\vec{\boldsymbol{\epsilon}} : \vec{\Delta\boldsymbol{\epsilon}} > 0.9$ can be used, wherein by definition $\boldsymbol{\epsilon} = 0$ at the beginning of the loop and $\Delta\boldsymbol{\epsilon}$ is measured from the recent recorded strain.
3. *Pseudo-creep mode* calculates stress increments explicitly using (1) and (2). Before the first increment in this mode is executed the amplitude A_ϵ must be calculated (according to the steps presented in Section 3).

The explicit calculation is mesh sensitive due to the fact that the rate of pseudo-creep is a function of the *square* of the strain amplitude. As an illustration we consider the case of a one-dimensional strain amplitude field $\epsilon^{\text{ampl}} = (1 - x/2)$ for $0 < x < 2$, Figure 4. The conventional settlement Δs is a *linear* function

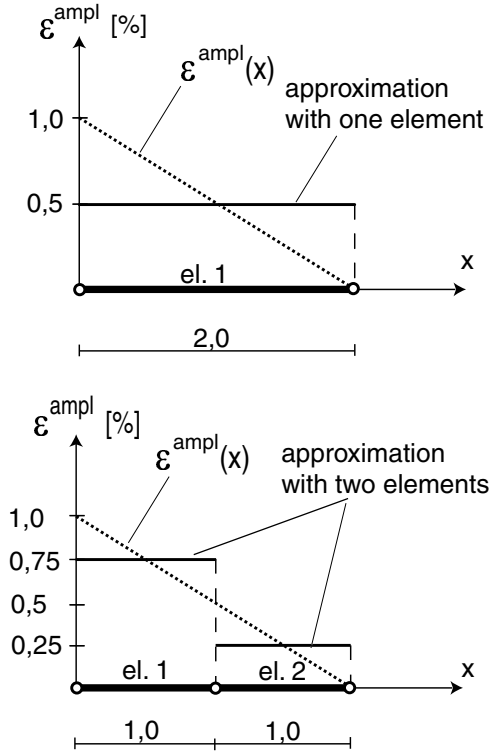

Figure 4. Mesh dependence of 'explicit' computation

of strain and therefore the number of constant-strain elements (step-like approximation of strain) has little effect on the integral value Δs. The rate of cyclic accumulation is dependent on the square of the amplitude and thus the approximation of the amplitude is improved with the number of constant-strain elements and we obtain different values of settlement. With reference to Figure 4 the accumulation

$$\Delta s = \int_0^L C \left(\epsilon^{appr}\right)^2 \mathrm{d}x \tag{32}$$

results in displacements $\Delta s^{(1)} = \frac{1}{2}C$ and $\Delta s^{(2)} = \frac{10}{16}C$ for a one-element and a two-element discretization, respectively. In practical FE calculations this problem was extensively studied by Hammami (2003) showing that the effect of discretisation is of secondary importance.

The control cycles switched on during the pseudo-creep mode turned out to improve significantly the results, especially for complicated boundary value problems. If no significant redistribution of stress is expected (e.g. FE simulation of laboratory tests) the control cycles can be less frequent.

6 FINITE ELEMENT CALCULATION

The proposed material model was used to calculate a centrifuge model test which was performed at our institute (Helm et al. 2000). In the model test a strip foundation on a freshly pluviated dense fine sand (ϱ_s = 2,66 g/cm^3, $e_{\min}$ = 0.583, $e_{\max}$ = 0.914, d_{50} = 0.21 mm, U = 1.95, $I_D \approx 0.90$) was cyclically loaded between 4 % and 47 % of the static bearing capacity σ_B = 345 kPa. ($\sigma_{\min}$ = 13.6 kPa, $\sigma_{\max}$ = 163.8 kPa, σ^{av} = 88.7 kPa). The test was performed at an acceleration level of n = 20g. The geometry of the prototype as well as the load function and the soil parameters are shown in Figure 5. For technical reasons the foundation was placed on the sand surface without embedding. The sinusoidal load was applied with a frequency of 0.44 Hz (prototype).

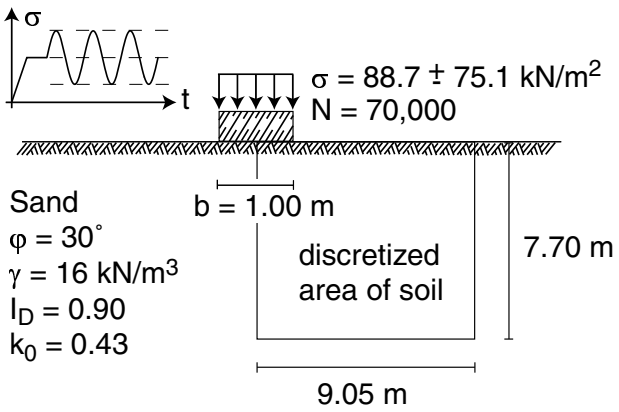

Figure 5. Geometry and soil parameters of the centrifuge model test

Figure 6 presents the obtained stress - settlement loops (prototype) for selected cycle numbers N. A mean amplitude of vertical displacement of s^{ampl} = 0.80 mm was measured. The application of σ^{av} lead to

a settlement of 1.4 cm below the middle of the foundation. After the irregular cycle a settlement of 2.5 cm remained. During the subsequent 100,000 regular cycles the accumulated settlement increased towards s^{acc} = 7.3 cm. The deformations of the foundation subsoil during cyclic loading were monitored with a video camera. Small layers of dyed sand were used in order to ease the observations. Figure 7 presents photographs before cyclic loading and after the application of 70,000 cycles. The foundation was slightly rotated. Zones of localized deformation at the edges of the foundation were observed.

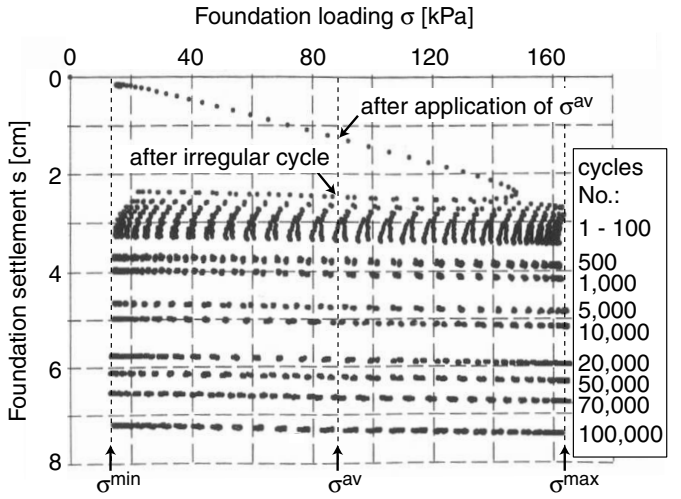

Figure 6. Foundation settlement as a function of the number of cycles

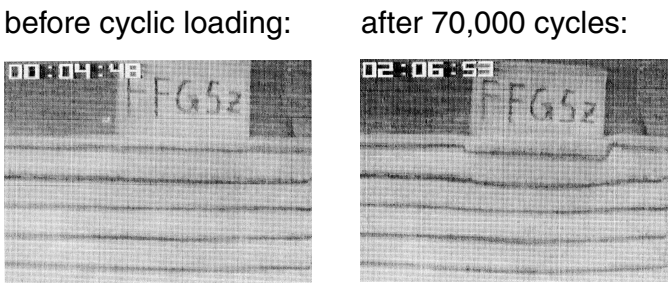

Figure 7. Photos of the centrifuge model before and after cyclic loading

The model test was calculated using the finite element program ABAQUS with the material model implemented in the user subroutine UMAT. Although the model test was performed on a fine sand the material parameters of the medium sand used for the derivation of the material model were taken for the calculation since the parameters were determined only for medium sand yet. No initial structural accumulation was assumed, g_0^A = 0, which seems reasonable for tests performed on freshly pluviated sand. The parameters of the intergranular strains in the hypoplastic material model (Niemunis 2003) used in the implicit calculation were chosen such that the amplitude of settlement s^{ampl} of the model test was reproduced. Only the right part of the halfspace under the foundation (9.05 × 7.70 m) was discretized with 4,000 four-nodal quadrangular elements.

Figure 8a presents the resulting field of the strain amplitude $\varepsilon^{\text{ampl}}$. The deformations concentrated near the foundation, thus not the whole discretised sector is shown. The field of the settlement s after 100,000 cycles is presented in Figure 8b. The application of σ^{av} lead to s = 0.30 cm and after the irregular cycle a settlement of 0.59 cm remained. Thus, the residual deformations in the implicit calculation were much less than in the model test (possibly due to surface imperfections). After 100,000 cycles a total settlement of s = 5.18 cm was calculated below the middle of the foundation. In Figure 9 the settlement of the middle of the foundation s is plotted versus the number of cycles N. Only the accumulation of deformations during the regular cycles is shown in Figure 9 and N = 1 means after the irregular cycle. The curves $s(N)$ from the calculation and the model test are compared. Although the settlements up to the end of the irregular cycle are quite different the subsequent curve $s(N)$ of the FE calculation fits the model test data satisfactory. While in the model test an accumulation of s^{acc} = 4.8 cm was observed during the regular cycles the FE calculation predicts s^{acc} = 4.0 cm.

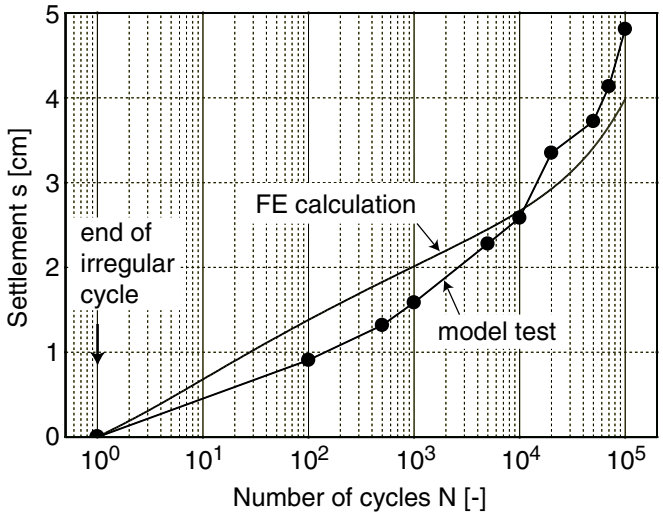

Figure 9. Accumulation of foundation settlement during the regular cycles: FE calculation versus model test

It has to be stated that the calculation presented in the Figures 8 and 9 does not consider yet the recent experimental finding that the volumetric part of the strain loop influences the accumulation rate (see CPMX), i.e. the strain amplitude A_ε was calculated ignoring the volumetric part of the strain loop (see the calculation schemes in Niemunis 2003, Niemunis et al. 2003, Triantafyllidis et al. 2003). The prediction of the accumulated settlement may become even more precisely if the amplitude A_ε is calculated via the modified scheme presented in Section 3. Further calculations considering the volumetric portion of the

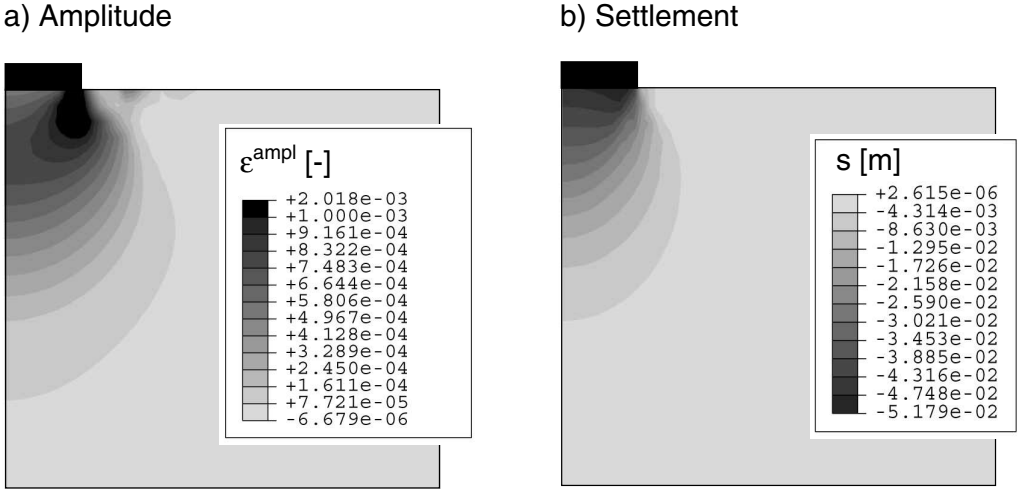

Figure 8. *a) Field of strain amplitude $\varepsilon^{\text{ampl}}$, b) Field of accumulated settlement s^{acc} after N = 100,000 cycles*

strain loop will follow.

7 ACKNOWLEDGEMENTS

The authors are grateful to DFG (German Research Council) for the financial support. This study is a part of the project A8 "Influence of the fabric changes in soil on the lifetime of structures" of SFB 398 "Lifetime oriented design concepts".

8 APPENDIX

Vectors and tensors are distinguished by bold typeface, for example $\mathbf{T}, \mathbf{v}$ or in sans serif font (e.g. E). The symbol $\cdot$ denotes multiplication with one dummy index (single contraction), e.g. the scalar product of two vectors can be written as $\mathbf{a}\cdot\mathbf{b} = a_k b_k$. Multiplication with two dummy indices (double contraction) is denoted with a colon, e.g. $\mathbf{A} : \mathbf{B} = \mathrm{tr}\,(\mathbf{A}\cdot\mathbf{B}^T) = A_{ij}B_{ij}$, wherein $\mathrm{tr}\,\mathbf{X} = X_{kk}$ reads trace of a tensor. Analogously we may define double colon :: to quadruple contraction with four dummy indices. We introduce two fourth order unit tensors $I_{ijkl} = \frac{1}{2}(\delta_{ik}\delta_{jl} + \delta_{il}\delta_{jk})$ and $J_{ijkl} = \delta_{ik}\delta_{jl}$. The brackets $\| \quad \|$ denote the Euclidean norm. The deviatoric part of a tensor is denoted by an asterisk, e.g. $\mathbf{T}^* = \mathbf{T} - \frac{1}{3}\,\mathbf{1}\mathrm{tr}\,\mathbf{T}$, wherein $(\ \mathbf{1})_{ij} = \delta_{ij}$ corresponds to the Kronecker's symbol. Dyadic multiplication is written *without* $\otimes$, e.g. $(\mathbf{ab})_{ij} = a_i b_j$ or $(\mathbf{T}\ \mathbf{1})_{ijkl} = T_{ij}\delta_{kl}$. Positively proportional quantities are denoted by tilde, e.g. $\mathbf{T} \sim \mathbf{D}$. Normalized quantities are denoted by arrow and tensors divided by their traces are denoted with hat, for example $\vec{\mathbf{D}} = \mathbf{D}/\|\mathbf{D}\|$ with $\vec{\mathbf{0}} = \ \mathbf{0}$, and $\hat{\mathbf{T}} = \mathbf{T}/\mathrm{tr}\,\mathbf{T}$. The sign convention of general mechanics with *tension positive* is obeyed. The superposed dot, $\dot{\square}$, denotes the material rate (with respect to N) and the superposed circle $\mathring{\square}$ denotes the Jaumann rate.

Only effective stresses $\mathbf{T}$ are used. In place of the popular Roscoe's variables

$$p \quad = -\frac{T_1+T_2+T_3}{3}; \quad q = -T_1 + \frac{T_2+T_3}{2}$$

$$D_v \quad = -D_1 - D_2 - D_3; \quad D_q = -\frac{2D_1 - D_2 - D_3}{3}$$

we prefer to use the 'normalized' isomorphic variables (Niemunis 2003)

$$P = \sqrt{3}p, \ \ Q = \sqrt{\frac{2}{3}}q, \tag{33}$$

$$D_P = \frac{1}{\sqrt{3}}D_v, \ \ D_Q = \sqrt{\frac{3}{2}}D_q \tag{34}$$

in order to preserve orthogonality. Note that $P^2 = \|\frac{1}{3}\,\mathbf{1}\mathrm{tr}\,\mathbf{T}\|^2$; $Q^2 = \|\mathbf{T}^*\|^2$ and $D_P^2 = \|\frac{1}{3}\,\mathbf{1}\mathrm{tr}\,\mathbf{D}\|^2$; $D_Q^2 = \|\mathbf{D}^*\|^2$ hold. We also use the basic invariants of the stress tensor: $I_1 = \mathrm{tr}\,\mathbf{T}$, $I_2 = [\mathbf{T} : \mathbf{T} - (\mathrm{tr}\,\mathbf{T})^2]/2$ and $I_3 = \det\mathbf{T}$

In the text we use a particular version (Wolffersdorff 1996, Wolffersdorff 1997, Niemunis 2003) of the hypoplastic constitutive model. Although the presentation of this model is outside the scope of the present paper we enclose (without comments) the equations necessary to formulate our explicit accumulation model.

$$a \quad = \quad \frac{\sqrt{3}(3-\sin\varphi_c)}{2\sqrt{2}\sin\varphi_c} \tag{35}$$

$$F \quad = \quad \sqrt{\frac{1}{8}\tan^2\psi + \frac{2-\tan^2\psi}{2+\sqrt{2}\tan\psi\cos 3\theta}}$$

$$-\frac{1}{2\sqrt{2}}\tan\psi\ , \tag{36}$$

wherein

$$\tan\psi = \sqrt{3}\|\hat{\mathbf{T}}^*\| \quad , \tag{37}$$

$$\cos 3\theta = -\sqrt{6}\,\frac{\mathrm{tr}\,(\hat{\mathbf{T}}^* \cdot \hat{\mathbf{T}}^* \cdot \hat{\mathbf{T}}^*)}{\left[\hat{\mathbf{T}}^* : \hat{\mathbf{T}}^*\right]^{3/2}} \tag{38}$$

REFERENCES

Baligh, M. & Whittle, A. 1987. Soil models and design methods. In *Geotechnical Design: Design Methods and Parameters, Conference, Politecnico di Torino*.

Barksdale, R. 1972. Laboratory evaluation of rutting in base course materials. In *Third International Conference on Structural Design of Asphalt Pavements* 3: 161-174.

Bouckovalas, G., Whitman, R. & Marr, W. 1984. Permanent displacement of sand with cyclic loading. *Journal of Geotechnical Engineering* 110(11): 1606-1623.

Ekberg, A. 2000. Rolling contact fatigue of railway wheels. Ph. D. thesis, Chalmers University of Technology, Solid Mechanics.

Gotschol, A. 2002. Ver¨anderlich elastisches und plastisches Verhalten nichtbindiger B¨oden und Schotter unter zyklisch-dynamischer Beanspruchung. Ph. D. thesis, Universit¨at GH Kassel.

Gudehus, G. 1996. A comprehensive constitutive equation for granular materials. *Soils and Foundations* 36(1): 1-12.

Hammami, M. 2003. Numerische Fehler bei der expliziten FE-Berechnung der Verdichtbarkeit von Sand infolge zyklischer Belastung. Diploma thesis, Institute of Soil Mechanics and Foundation Engineering, Ruhr-University Bochum.

Helm, J., Laue, J. & Triantafyllidis, Th. 2000. Untersuchungen an der RUB zur Verformungsentwicklung von B¨oden unter zyklischen Beanspruchungen. In Th. Triantafyllidis (ed.), *Beiträge zum Workshop: Böden unter fast zyklischer Belastung: Erfahrungen und Forschungsergebnisse, Bochum*, Report No. 32: 109-133.

Hornych, P., Corte, J. & Paute, J. 1993. Étude des d´eformations permanentes sous chargements r´ep´et´es de trois graves non trait´ees. *Bulletin de Liaison des Laboratoires des Ponts et Chaussées* 184: 77-84.

Khedr, S. 1985. Deformation characteristics of granular base course in flexible pavements. *Transportation Research Record* 1043: 131-138.

Kolymbas, D. 2000. Introduction to Hypoplasticity. In: *Advances in Geotechnical Engineering and Tunneling* 1, Balkema.

Lentz, R. & Baladi, G. 1981. Constitutive equation for permanent strain of sand subjected to cyclic loading. *Transportation Research Record* 810: 50-54.

Marr, W. & Christian, J. 1981. Permanent displacements due to cyclic wave loading. *Journal of the Geotechnical Engineering Division ASCE* 107(GT8): 1129-1149.

Martin, G., Finn, W. & Seed, H. 1975. Fundamentals of liquefaction under cyclic loading. *Journal of the Geotechnical Engineering Division ASCE* 101(GT5): 423-439.

Matsuoka, H. & Nakai, T. 1982. A new failure for soils in three-dimensional stresses. In *Deformation and Failure of Granular Materials, Proc. IUTAM Symp., Delft.*: 253-263.

Miner, M. 1945. Cumulative damage in fatigue transactions. *Journal of the Engineering Mechanics Division ASME*67.

Niemunis, A. 2000. Akkumulation der Verformung infolge zyklischer Belastung des Bodens - numerische Strategien. In Th. Triantafyllidis (ed.), *Beiträge zum Workshop: Böden unter fast zyklischer Belastung: Erfahrungen und Forschungsergebnisse, Bochum*, Report No. 32: 1-20.

Niemunis, A. 2003. Extended hypoplastic models for soils. Report No. 34, Institute of Soil Mechanics and Foundation Engineering, Ruhr-University Bochum.

Niemunis, A., Wichtmann, T. & Triantafyllidis, Th. 2003. Compaction of freshly pluviated granulates under uniaxial and multiaxial cyclic loading. In *XIIIth European Conference On Soil Mechanics and Geotechnical Engineering: Geotechnical problems with man-made and man-influenced grounds, Prag*: 855-860.

Papadopoulos, I. 1994. A new criterion of fatigue strength for out-of-phase bending and torsion of hard metals. *International Journal of Fatigue* 16: 377-384.

Paute, J., Jouve, P. & Ragneau, E. 1988. Modèle de calcul pour le dimensionnement des chauss´ees souples. *Bulletin de Liaison des Laboratoires des Ponts et Chaussées* 156: 21-36.

Sagaseta, G., Cuellar, V. & Pastor, M. 1991. Cyclic loading. In *Deformation of soils and displacements of structures, Proceedings of the 10-th ECSMFE in Firenze, Italy* 3: 981-999.

Sawicki, A. 1987. An engineering model for compaction of sand under cyclic loading. *Engineering Transactions* 35: 677-693.

Sawicki, A. & Świdzi´nski, W. 1989. Mechanics of a sandy subsoil subjected to cyclic loadings. *International Jounal for Numerical and Analytical Methods in Geomechanics* 13: 511-529.

Sawicki, A. 1991. Mechanika grunt´ow dla obciążen cyklicznych, Gda´nsk: Wydawnictwo IBW PAN.

Suiker, A.S.J. 1998. Fatigue behaviour of granular materials. Technical Report 7-98-119-3, Delft University of Technology, Faculty of Civil Engineering.

Suiker, A.S.J. 1999. Static and cyclic loading experiments on non-cohesive granular materials. Report No. 1-99-DUT-1, TU Delft.

Sweere, G. 1990. Unbound granular bases for roads. Ph. D. thesis, Delft University of Technology, Netherlands.

Triantafyllidis, Th., Wichtmann, T. & Niemunis, A. 2003. Explicit accumulation model for granular materials under multiaxial cyclic loading. In *6th International Workshop On Mathematical Methods In Scattering Theory and Biomechanical Engineering, Ioannina*. World Scientifi c.

Triantafyllidis, Th., Wichtmann, T. & Niemunis, A. 2004. On the determination of cyclic strain history. In *International Conference on Cyclic Behaviour of Soils and Liquefaction Phenomena, Bochum, 31 March - 02 April*. Balkema.

Vuong, B. 1994. Evaluation of back-calculation and performance models using a full scale granular pavement tested with the accelerated loading facility (alf). In *Proceedings 4 th International Conference on the Bearing Capacity of Roads and Airfields, Minneapolis*: 183-197.

Wichtmann, T., Niemunis, A. & Triantafyllidis, Th. 2004a. Accumulation of strain in sand due to cyclic loading under drained triaxial conditions. *Soils & Foundations (submitted)*.

Wichtmann, T., Niemunis, A. & Triantafyllidis, Th. 2004b. Strain accumulation in sand due to drained uniaxial cyclic loading In *International Conference on Cyclic Behaviour of Soils and Liquefaction Phenomena, Bochum, 31 March - 02 April*. Balkema.

Wichtmann, T., Niemunis, A. & Triantafyllidis, Th. 2004c. The effect of volumetric and out-of-phase cyclic loading on strain accumulation. In *International Conference on Cyclic Behaviour of Soils and Liquefaction Phenomena, Bochum, 31 March - 02 April*. Balkema.

Wolff, H. & Visser, A. 1994. Incorporating elasto-plasticity in granular layer pavement design. In *Proceedings of Institution of Civil Engineers Transport* 105: 259-272.

Wolffersdorf, P.-A. v. 1997. Verformungsprognosen f¨ur St¨utzkonstruktionen. Habilitation. Institut f¨ur Boden- und Felsmechanik der Universit¨at Karlsruhe. Report No. 141.

Wolffersdorff, P.-A. v. 1996. A hypoplastic relation for granular materials with a predefined limit state surface. *Mechanics of Cohesive-Frictional Materials* 1: 251-271.